euspen's 16th International Conference & Exhibition, Nottingham, UK, May 2016
www.euspen.eu

On machine polishing of ultraprecision diamond ground aspherical surfaces on multispectral CVD ZnS lens

Zhimin Rao, Qingliang Zhao, Bing Guo

Center for Precision Engineering, School of Mechatronics Engineering, Harbin Institute of Technology, Harbin 150001, China

raozm@hit.edu.cn

Abstract
For the aspheric machining of zinc sulphide, ultraprecision diamond grinding and the CNC sub-aperture polishing were applied on the same machine tool. After ultraprecision diamond grinding, CNC sub-aperture polishing was performed successively without removing the part from workpiece spindle. For making the on machine polishing realized, the tool influence function (TIF) and dwell-time map need to be achieved. Firstly, the TIF for the process of computer-controlled polishing with soft polishing wheel was theoretically presented based on the Preston equation. For establishing the interfacial pressure distribution model, the Winkler elastic foundation was introduced to model the polishing wheel in the contact zone. A series spot experiments were conducted to obtain the removal spot statistical properties for establishing the TIF. Secondly, the dwell-time map was calculated through formulating the form correction into the matrix form. For the axis-symmetrical part, the material removal distribution could be calculated by one dimension TIF in a polar coordinate system. To achieve the convergence between actual and simulated removal profile, the TIF matrix need to be corrected by multiplying an adjusting matrix before form correction. Depending on the on machine form error measure equipment, the part error map could be obtained to work out the dwell-time map. After on machine polishing, the ultraprecision ground aspherical surfaces of the CVD zinc sulphide lens become smoother while the form accuracy does not deteriorate. the experimental result indicate that the on machine polishing technique of ultraprecision diamond ground aspherical CVD ZnS lens was achieved to fulfil the high efficiency machining of infrared aspherical lens which are hard- to-machine via diamond turning .

Keywords: on machine polishing, aspherical ZnS lens, TIF,dwell-time map, surface roughness, form accuracy

1. Introduction

As the increasing employment of aspheric and free forms with high surface form accuracy, low surface roughness, and free defects, many classical deterministic sub-aperture polishing techniques have been developed. These techniques include magnetorheological finishing (MRF) [1, 2], 'Precessions' polishing [3, 4], Ultra Form Finishing (UFF) [5, 6], fluid jet polishing (FJP) [7, 8], ion beam figuring (IBF) [9], stressed-lap polishing [10], etc. Generally, CNC sub-aperture polishing process was applied after deterministic microgrinding and the two manufacturing process were performed on two different styles of machine tools respectively. The multiple machine tool that could perform grinding and polishing had not appeared yet. Actually the two independent process could be performed on the same machine tool with appropriate alteration. In this paper, a polishing module was mounted on a deterministic microgrinding tool for achieving polishing. For making the on machine polishing realized, the tool influence function (TIF) was studied and dwell-time map was calculated for the particular machine tool configuration. By aspherical profile polishing, the TIF and dwell-time map algorithm was verified.

2. Machine tool configuration for polishing

For realizing the on machine polishing, the polishing module was installed on a homemade four-axis precision grinding machine tool, as shown in Figure 1, and the control system configuration was finished correspondingly.

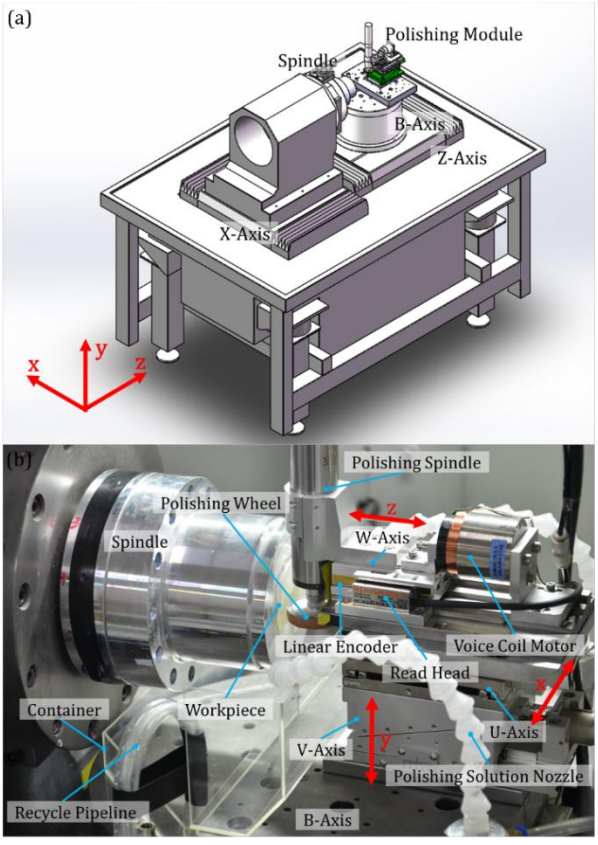

Figure 1. Machine tool configuration for polishing (a) 4-axis homemade grinding machine tool configuration. (b) Polishing module.

3 Fundamental model

3.1. Tool Influence function

The material removal rate is described by Preston in 1927. The locally relevant generalized form of Preston's equation can be expressed as,

$$MRR(x,y) = C_P p(x,y)^{\alpha} v(x,y)^{\beta} \tag{1}$$

According to machine tool configuration, the relative velocity expressed as,

$$v_{rel} = \sqrt{(\omega_w r_w \cos(\gamma) - \omega_p y)^2 + (\omega_p x)^2 + (\omega_w r_w \sin(\gamma))^2} \tag{2}$$

For the contact of polishing wheel and part, contact pressure distribution was expressed as [11],

$$p(x,y) = \begin{cases} \dfrac{p_{\max}}{R_w - \sqrt{R_w^2 - r_c^2}} \left(\dfrac{0.409 y^2}{r_c^2} + 1\right)\left[-\sqrt{R_w^2 - r_c^2}\right. \\ \dfrac{p_{\max}}{R_w - \sqrt{R_w^2 - r_c^2}} \left(\dfrac{0.409 y^2}{r_c^2} + 1\right)\left[-\sqrt{R_w^2 - r_c^2}\right. \\ \left. + r_c \sqrt{\dfrac{R_w^2}{r_c^2} - \dfrac{x^2}{a'^2} - \dfrac{y^2}{b^2}}\right] \quad , x > 0 \,\&\, \dfrac{x^2}{a'^2} + \dfrac{y^2}{b^2} \le 1 \\ \left. + r_c \sqrt{\dfrac{R_w^2}{r_c^2} - \dfrac{x^2}{a^2} - \dfrac{y^2}{b^2}}\right] \quad , x \le 0 \,\&\, \dfrac{x^2}{a^2} + \dfrac{y^2}{b^2} \le 1 \end{cases} \tag{3}$$

By experiments, we can obtain these parameters' values which relate to the TIF including C_P, $p_{\max}$, α and β.

For the axisymmetric part, the tool influence function could be expressed in polar coordinate system(r, θ) as follows,

$$MRR'(r, x_w) = \frac{1}{2\pi} \int_{\Theta} MRR(x(r,\theta), y(r,\theta), x_w) d(\theta) \tag{4}$$

The TIF of the soft wheel polishing had been established.

3.2. TIF matrix and dwell time map calculation

The radial removal depth could be expressed in matrix form [12] as follows,

$$Rdepth_m = TIF_{m \times n} \cdot T_n \tag{5}$$

$TIF_{m \times n}$ is the matrix of TIF, and its (i, j)th element was given by Eq. (4). The related parameters' values of TIF were confirmed, then the TIF matrix was determined, the normalize results as shown in Figure 2.

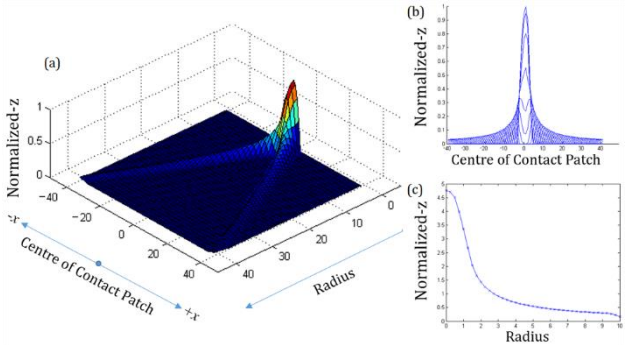

Figure 2. TIF matrix simulation. (a) Removal function matrix. (b) Removal distribution at each radius. (c) Material removal of every radius.

An optimized method was used to obtain the dwell time map for Eq. (5). The calculated dwell time map combining with the predefined tool path was applied to finish aspheric profile polishing.

4. Aspherical profile polishing results

In order to minimize the variations of tool influence function during aspherical surface polishing, it was designed to align the tool normal with part normal by controlling B-axis when the tool moving on the part profile and the geometry of the polishing tool motion was shown in Fig. 3.

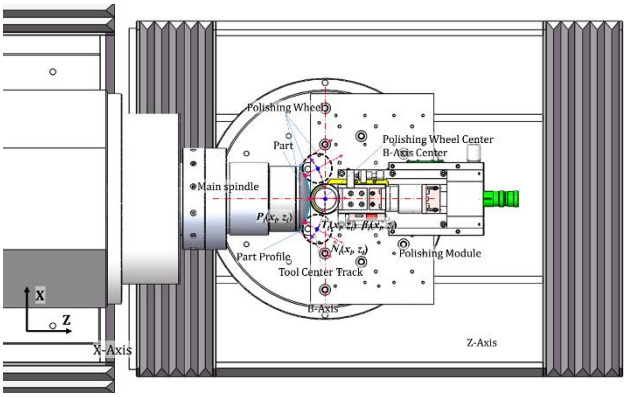

Figure 3. Geometry of the polishing tool motion in xoz plane.

A zinc sulphide aspherical profile was polished after deterministic microgrinding. Manufacturing profile was measured by a LuphoScan metrology platform (LuphoScan 420) and its basic measurement principle is a scanning of rotational symmetric objects surface with the MWLI point sensor (MWLI-multi-wave-length interferometer) and four precision stages. The results was displayed by Zygo MetroPro, as shown in Figure 4. After microgrinding, the aspheric profile form error PV value was 617.3 nm and RMS value was 112.1 nm. After soft wheel polishing, the form error PV value was 644.6 nm and RMS value was 105.2 nm.

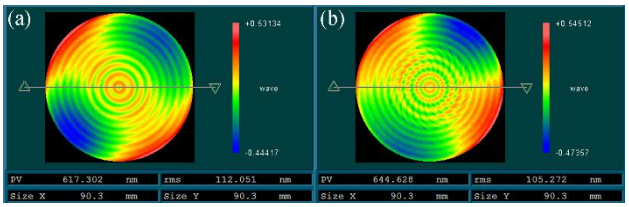

Figure 4. Manufacturing results. (a) Surface error after microgrinding. (b) Surface error after soft wheel polishing.

5. Conclusion

For make on machine polishing realized, the soft wheel polishing module was installed on the homemade grinding machine tool. Tool influence function and dwell time map were obtained for manufacturing aspherical profile by this particular machine tool configuration. The manufacturing results revealed that the form accuracy did not deteriorate badly after soft wheel polishing. The on machine polishing was achieved and the future work will focus on the way to improve the form accuracy.

References

[1] D. Golini, S. Jacobs, W. Kordonski, and P. Dumas 1997 *Proc. SPIE* **CR67**, 251–274.

[2] J. C. Lambropoulos, C. L. Miao, and S. D. Jacobs 2010 *Opt. Express* **18**(19), 19713–19723.

[3] D. Walker, D. Brooks, A. King, R. Freeman, R. Morton, G. McCavana, and S.-W. Kim 2003 *Opt. Express* **11**, 958-964.

[4] D. D. Walker, R. Freeman, R. Morton, G. McCavana, and A. Beaucamp 2006 *Opt. Express* **14**, 11787-11795.

[5] C. Bouvier, S. M. Gracewski, and S. J. Burns 2006 OSA Technical Digest (CD) (Optical Society of America,), OFME4.

[6] C. Bouvier, S. M. Gracewski and S. J. Burns 2007 *Proc. SPIE* **6545**, 65450R.

[7] O. W. Fähnle, H. van Brug, and H. J. Frankena 1998 *Appl. Opt.* **37**, 6771-6773.

[8] Z. Li, S. Li, Y. Dai, and X. Peng 2010 *Appl. Opt.* **49**, 2947-2953.

[9] T. W. Drueding, T. G. Bifano, and S. C. Fawcett 1995 *Precis. Eng.* **17**, 10-21

[10] H. Martin, D. Anderson, J. R. P. Angel, R. H. Nagel, S. C. West, and R. S. Young 1990 *Proc. SPIE* **1236**, 682–690.

[11] Z. Rao, B. Guo, and Q. Zhao 2015 *Appl. Opt.* **54**, 8091-8099

[12] C. L. Carnal, C. M. Egert, K. W. Hylton 1992, *Proc. SPIE* **1752**, 54-62